Applied Catalysis B: Environmental 176–177 (2015) 315–324

Contents lists available at ScienceDirect

Applied Catalysis B: Environmental

journal homepage: www.elsevier.com/locate/apcatb

Selective biomolecular photocatalytic decomposition using peptide-modified TiO_2 nanoparticles

Justin R. Smith[a,1], Kensey R. Amaya[a,1], Rudi T. Bredemeier[a], Scott Banta[b], Donald M. Cropek[a,*]

[a] U.S. Army Engineer Research and Development Center, Construction Engineering Research Laboratory (CERL), Champaign, IL 61822, USA
[b] Department of Chemical Engineering, Columbia University, 500 W 120th Street, New York, NY 10027, USA

ARTICLE INFO

Article history:
Received 27 November 2014
Received in revised form 12 February 2015
Accepted 31 March 2015
Available online 2 April 2015

Keywords:
Photocatalysis
TiO_2
Surface modification
Affinity peptides
Protein degradation

ABSTRACT

Titanium dioxide (TiO_2) is a photocatalyst widely used for the degradation of inorganic and organic contaminants in the environment; however, its lack of chemical specificity can be a particular limitation since every species in solution, including valued, innocuous, and deactivating compounds, will be degraded or deleterious to the process. Here, we describe a means to target the photocatalysis by surface modification of nanoparticulate TiO_2 with a 13 amino acid streptavidin binding peptide (SBP) for the selective degradation of streptavidin, a 60 kDa tetrameric protein. Modification of the TiO_2 surface with the affinity peptide was confirmed by fourier transform infrared spectroscopy (FTIR), UV/Vis absorbance, and secondary ion mass spectrometry (SIMS), while streptavidin binding and affinity to bound SBP were tested using fluorescently tagged antibodies against streptavidin. Results show that the SBP retains its affinity toward streptavidin after immobilization onto TiO_2. Photodegradation studies using the visible region of simulated solar radiation ($\geq$360 nm) showed rapid streptavidin degradation by SBP–TiO_2 both in solution and while the photocatalyst was immobilized as a thin film on a glass substrate. In contrast, photocatalytic degradation of a non-target protein, lysozyme, was inhibited by the SBP monolayer and incompletely degraded, indicating that surface modification with biorecognition agents can control and modulate the photocatalytic process. Moreover, after extended illumination (3 h), the SBP-modified TiO_2 surface retained its ability to bind streptavidin demonstrating that the SBP is stable at the TiO_2 surface and that the SBP–TiO_2 surface is reusable. These results indicate that the modification of TiO_2 with covalently bound peptide recognition moieties offers the ability to selectively degrade target proteins of interest, leaving non-target components largely unaffected.

Published by Elsevier B.V.

1. Introduction

Heterogeneous photocatalysis presents one of the most powerful and inexpensive means for water and air decontamination, especially when exploiting solar radiation as the illumination source and immobilizing the catalyst to obviate the need to filter and recollect the particulates. Titanium dioxide (TiO_2 or titania) is one of the best and most widely studied metal oxide photocatalysts due to its low cost, non-toxicity, stability, lack of needed additives, and relatively small band gap [1–8]. Through several decades, it has found use in a variety of applications to degrade myriad contaminants in both air and water phase [2–13] and is mature enough to play a central role in commercial self-cleaning products [[14] and references therein]. Its non-selective targeting of a wide breadth of molecules is an asset to its powerful flexibility to decontaminate media. This includes degradation of organic molecules such as polychlorinated biphenyls [15], nitroaromatic explosives [9–12], hydrocarbons [16], reduction of heavy metals [17–19], and even cytotoxicity toward pathogens [20–23]. While new applications of TiO_2 photocatalysts are continually documented, current research focuses on several of its perceived weaknesses, *i.e.*, preventing exciton recombination through rapid and long distance charge separation [15], narrowing the excitation band gap by extending the absorption spectrum into the visible through atomic doping and dye-catalyst hybrid particles [8], reduction of surface poisoning

Abbreviations: SBP, streptavidin binding peptide; FTIR, fourier transform infrared spectroscopy; SIMS, secondary ion mass spectrometry; PDMS, polydimethylsiloxane; PBS, phosphate buffered saline; BSA, bovine serum albumin.

* Corresponding author at: P.O. Box 9005, Champaign, IL 61826-9005, USA. Tel.: +1 217 373 6737; fax: +1 217 373 7222.
E-mail address: Donald.M.Cropek@usace.army.mil (D.M. Cropek).

[1] These authors contributed equally to this manuscript.

http://dx.doi.org/10.1016/j.apcatb.2015.03.060
0926-3373/Published by Elsevier B.V.

[24], and introducing degradation selectivity through surface modification [25,26].

Surface modification by organic constituents can manipulate several interesting functions of the photocatalyst behavior. For instance, functionalizing the surface of TiO_2 with L-hydroxyproline significantly increases rhodamine B degradation over bare TiO_2 alone by acting as a hole trap to prevent exciton recombination [27]. Rajh et al. has shown that modifying the TiO_2 surface with cysteine initiates reduction of heavy metals to the zero-valent state [28], while Skubal et al. show that thiolactic acid modified TiO_2 behaves the same way for cadmium [18]. Li et al. used 5-sulfosalicylic acid modified TiO_2 to enhance the degradation efficiency of *p*-nitrophenol through increased light absorptivity in the visible and increased nitrophenol adsorption onto the photocatalyst [29].

The ability to selectively target a single contaminant from a waste stream would represent an important advance in media treatment. The toxic or problematic component is frequently only a minor constituent in a complex mixed matrix of more concentrated, but less noxious compounds [25]. Selectively degrading only the single component minimizes the total waste stream treatment requirements and even allows for reuse of the remaining components. Selectivity can be introduced by controlling the mass transfer of the analyte to the catalyst, increasing the affinity of the analyte with the catalyst, or otherwise increasing the interaction time of the analyte with the reactive surface [25]. This has been previously accomplished by increasing the affinity interaction between the TiO_2 catalyst and pollutants *via* n-π or π-π interactions [30–33], donor–acceptor complexation [34], host-guest interactions [35,36], combining activated carbon sorbent with titania [37], or merely exploiting hydrophobic interactions [38,39]. As examples, Ranjit et al. illustrated that an *N*,*N*′-bipyridinium π-acceptor layer on TiO_2 has superior photocatalytic activity to bare TiO_2 for decomposition of π-donor substrates such as 1,4-dimethoxybenzene, 1,2-dimethoxybenzene, and indole due to formation of supramolecular π donor–acceptor complexes [34]. Ghosh-Mukerji et al. showed that immobilizing β-cyclodextrin near the TiO_2 active surface combined physisorption of appropriately sized guest molecules with controlled diffusion to the photocatalytic site leading to degradation rate increases [36]. Several results have been published using either a molecularly imprinted layer on the titania [40] or conversely, using the titania as a component of the molecularly imprinted gel to create template cavities for specific analytes [41]. In this way, chlorophenols and azobenzene carboxylic acids have been targeted. A particularly interesting example of using a relatively large biorecognition agent is shown by Ogino et al. where titania is modified with an anti-estradiol antibody through a polyacrylic acid linker [26]. The antibody improved the degradation rate by increasing the residence time of the target estradiol near the titania surface, however, this construct did not demonstrate selectivity nor did the authors demonstrate antibody stability upon illumination.

Our previous work demonstrated this concept by modifying TiO_2 with surface bound arginine to enhance the photocatalytic selectivity toward nitroaromatic compounds (*e.g.*, explosives) from a solution also containing phenol, an easily oxidized compound [31]. The amino acid was bound in a very stable bidentate configuration through the carboxylate moiety to incompletely coordinated titanium atoms at the nanoparticle surface. The arginine prevented recombination by acting as a hole trap, initiated n–p interactions, and slightly extended the absorption spectrum of the hybrid photocatalyst into the visible region. Further, it shifted the degradation pathway of the nitrocompound from an oxidative mechanism to a reductive one, transforming nitro groups into amine groups. This culminated with a build-up of the amine compound, illustrating that, immediately upon target transformation, the by-product is effectively ignored by the arginine-modified TiO_2. This concept was extended to use other amino acids such as asparagine, serine, phenylalanine, and tyrosine bound to titania, all demonstrating photoreduction of nitrobenzene to aniline [42]. The research described here expands on our previous research to immobilize not just single amino acids but longer chain molecular recognition peptides to determine the ability of this modifier to increase the power and flexibility to selectively degrade a desired biomolecular target.

In this paper, we report the use of a 13-amino acid peptide sequence, streptavidin binding peptide (SBP), to modify the surface of TiO_2, thus imparting photocatalytic degradation selectivity toward streptavidin, a ~60 kDa protein. The modified TiO_2 was initially examined to verify the presence of the SBP layer. Thin films of the TiO_2 were used to determine the optimal concentration of surface SBP to maximize the amount of bound streptavidin. SBP-modified TiO_2 (SBP–TiO_2) was illuminated in both a thin film configuration and as a colloidal solution to verify the function and stability of the SBP monolayer for streptavidin affinity as well as to observe the extent of photocatalytic degradation of streptavidin. We further demonstrate photocatalytic degradation selectivity of SBP–TiO_2 by studying the photocatalysis of lysozyme, a protein with no known affinity for SBP. Our modification of the TiO_2 with a small stable biorecognition peptide for targeted photocatalysis is an initial step for using hybrid photocatalysts to degrade selected biological analytes in complex matrices.

2. Experimental

All chemicals and proteins were reagent grade from Sigma–Aldrich and used without further purification unless otherwise noted.

2.1. Photocatalyst preparation

Colloidal TiO_2 was prepared by dropwise addition of titanium (IV) chloride to ice cold water followed by dialysis against distilled water at 4 °C as previously described [28]. The mean particle size of the resultant TiO_2 was 45 Å as determined by Makarova et al. [30]. The concentration of TiO_2 was determined by dissolving the colloid in concentrated H_2SO_4 and measuring the resultant titanium peroxide complex spectrophotometrically at 410 nm [43,44]. The as-prepared solution of TiO_2 nanoparticles was close to 0.1 M and was stored at 4 °C until use. This colloidal solution was used directly in colloidal solution experiments or for formation of thin films.

Surface modification of the nanocrystalline colloidal TiO_2 with a synthesized streptavidin binding peptide (SBP, Genscript, Piscataway, NJ, 98.1% purity) was carried out by mixing equal volumes of TiO_2 (0.1 M) and SBP (5 mM in phosphate buffered saline (PBS), pH 7.4) for 24 h at room temperature in the dark. The SBP was a concatenation of a streptavidin recognition sequence, *Strep*-tag II (WSHPQFEK) [45], with a 5 residue linker (GSGSC). Before use, bare and surface-modified TiO_2 colloids were centrifuged and washed four times with twice the original volume with PBS (pH 7.4) followed by a final wash with 18.2 MΩ × cm MilliQ water to remove unbound SBP.

2.2. Titania dip coating

Quartz coverslips (Corning, Tewksbury, MA) were first cleaned in either piranha solution (3:1 concentrated sulfuric acid to 30% hydrogen peroxide) or 2% hellmanex (Mullheim, Germany), followed by plasma cleaning. The coverslips were subsequently dipped into the colloidal TiO_2 solution, removed at a rate of 10 cm/min, and then baked at 150 °C for 30 min. Thin film thickness was measured using the resultant interference fringes in the transmission spectrum over the 280–900 nm spectral range using a Cary

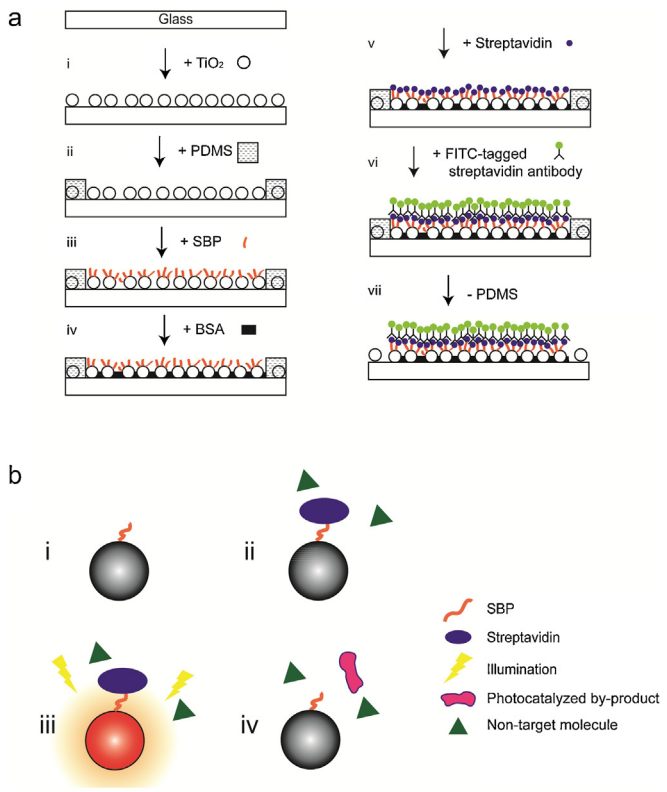

Fig. 1. (a) Schematic of steps for thin film TiO_2 deposition and modification on a glass coverslip, followed by fluorescent tagging of bound streptavidin. See text for details. (b) Schematic of illumination of modified TiO_2 in a colloidal suspension. (i) SBP-modified TiO_2, (ii) SBP-modified TiO_2 with streptavidin, (iii) sample is illuminated, and (iv) streptavidin is photocatalytically degraded while SBP remains intact on the surface of TiO_2. Non-target protein molecules are not attracted to the photocatalyst and are not degraded. Figure is not to scale and is a 2D representation of 3D space.

UV/Vis spectrophotometer (Agilent Technologies, Wilmington, DE) (Supplemental information, Fig. S1) [46,47]. The dip-coating and baking was repeated three times resulting in a coating thickness of about 10–15 nm based on the curve shown in Fig. S1.

TiO_2 coated coverslips were further prepared as shown in Fig. 1a. Slides were covered with a thin (~100 μm) layer of polydimethylsiloxane (PDMS) with 1 mm bore holes to create wells with exposed titania underlayers (Steps i and ii). Next, a solution of SBP (5 mM) was added to the wells and allowed to equilibrate for 24 h at room temperature in a dark, humid chamber (Step iii) to provide ample time for the SBP to bind to the TiO_2 layer. Unbound SBP was removed by washing the surface with phosphate buffered saline (PBS) with 0.1% Tween 20 followed by PBS alone. Bovine serum albumin (BSA), a known blocking agent which prevents non-specific adsorption, was then placed into each well to cover any potential remaining bare TiO_2 surfaces that were uncoated by SBP, as well as any possible bare glass substrate. The slide was incubated for 24 h, and then rinsed (Step iv) to remove excess BSA from the slide. Streptavidin solution (3 mg/mL in PBS, from *Streptomyces avidinii*) was placed into each well, left for 2 h to allow time for the streptavidin to bind to the SBP modified TiO_2, and then rinsed with PBS to remove any excess unbound streptavidin (Step v). For fluorescence experiments, a FITC-tagged anti-streptavidin antibody (ab7238, Abcam, Cambridge, MA) was added (1/100 dilution) and allowed to bind for 1 h (Step vi). This FITC-tagged antibody linked to streptavidin at the surface and thus served as a fluorescent indicator for affinity during thin film fluorescence experiments (described in detail below). The surface was then rinsed with PBS to remove excess and unbound antibody, and the PDMS overlayer was removed to expose the TiO_2 underlayer for better imaging (Step vii). A final wash with DI H_2O was done to remove any residual salt, and the coverslip was mounted to a glass slide (VWR, Randor, PA) with the antifade reagent ProLong Gold (Invitrogen, Grand Island, NY).

2.3. FTIR analysis

Samples were dried and mixed with KBr (1:1 by weight). FTIR measurements were performed on a Mattson Infinity Gold FTIR (Thermo Scientific, West Palm Beach, FL) equipped with a Spectra Tech. Inc. (Stamford, CT) diffuse reflectance accessory. Each spectrum was an average of 4096 scans and results are presented as Kubelka–Munk plots. To eliminate background peaks, samples for IR analysis were not blocked with BSA.

2.4. SIMS analysis

SIMS analysis was carried out on a TRIFT ToF-SIMS mass spectrometer (Physical Electronics, Chanhassen, MN, USA) equipped with a gold liquid metal ion source. The pulsed monoatomic Au primary ion source was operated at 22 keV, 2 nA, and the primary dose was kept below the static limit of 1×10^{13} primary ions cm^{-2} and positive secondary ions (m/z 0.1–2,000) were collected with charge compensation. The primary beam was raster-scanned across the surface, recording a mass spectrum for each pixel using WinCadence software (Physical Electronics, Chanhassen, MN). Mass spectra were collected from a 250 μm × 250 μm area and normalized to the total ion count prior to analysis. Imaging of 1 × 1 mm areas was performed with the built-in mosaic function with each image being composed of 16 distinct tiled images. Masses of interest are then selected from the spectrum with their intensities mapped and displayed in false color across the imaging area. All images were convolved once using the default settings in WinCadence and individually scaled to a relative intensity of 0–100%. Results of ToF-SIMS signal intensity with respect to SBP solution concentration (1 μM to 5 mM) were compared by selecting a region of interest and normalizing the ion spectra to the total ion count. This allowed the signal intensity of peaks representing SBP to be compared.

2.5. Thin film fluorescence

The fixed dip coated coverslips from Fig. 1a, step vii were analyzed using an IX-81 inverted fluorescence microscope (Olympus, Center Valley, PA) with MetaMorph Basic software (Molecular Devices, Sunnydale, CA). Fluorescent intensities were normalized across each experiment and measured using ImageJ [48].

2.6. Thin film illumination

A Cermax PE300BUV xenon lamp (Excelitas Technologies, Fremont, CA) was set on a raised platform 30 cm above an airtight round quartz cell. The cell was placed inside a crystallizing dish with circulating cool water using a water pump (Cole Palmer, Vernon Hills, IL). A 360 nm long pass filter (Newport, Irvine, CA) was placed between the lamp and the sample to reject UV irradiation while still allowing visible light to pass.

A modified TiO_2 coated slide was placed at the bottom of the round cell and DI water was added until the thin film was approximately 10–15 cm below the surface. The SBP-modified TiO_2 thin film with streptavidin attached (Fig. 1a, Step v) was illuminated for 3 h. The thin film sample was then rinsed with PBS and 0.1% Tween 20 followed by PBS alone. Next, BSA was added as a blocking agent to prevent non-specific protein binding onto any extant bare TiO_2 in subsequent steps and allowed to sit for 24 h. Analysis of the remaining surface groups after the 3 h illumination was done by adding streptavidin and FITC-tagged anti-streptavidin antibody,

or the FITC-tagged anti-streptavidin antibody alone. These samples were processed and analyzed by fluorescence microscopy as described above.

2.7. Colloidal illumination

A 1 mm quartz cell (Fisher Scientific, Pittsburgh, PA) was positioned beneath the xenon lamp previously described and illumination studies were performed for 3 h unless otherwise stated. A series of streptavidin standard solutions in PBS was prepared from 0 to 5 mg/mL to calibrate the HPLC peak areas (Supplemental information, Fig. S2) and the analytical limit of detection for streptavidin was determined to be 0.1 mg/mL. A streptavidin concentration of 3 mg/mL was used as the nominal concentration for degradation experiments, including a non-illuminated control sample as well as a photolysis experiment performed in the absence of any form of TiO_2. A lysozyme concentration of 1 mg/mL was used as a non-specific target protein for comparison. Photocatalysis was investigated by mixing a protein with bare TiO_2 or SBP–TiO_2 to form a colloidal suspension just prior to illumination.

2.8. HPLC analysis

Fifty microliter aliquots of the test samples were injected on an Alliance 2695 HPLC (Waters Corp., Milford, MA) at room temperature employing a Viva C18 column (Restek, Bellefonte, PA) and a photodiode array detector (Waters Corp.). Both proteins were best detected at their absorbance maximum of 280 nm. Separations used a solvent gradient starting at 95% (0.1% trifluoroacetic acid (TFA) in H_2O): 5% (0.1% TFA in acetonitrile (Fisher Scientific)) to a final ratio of 65%: 35% over 30 min at a flow rate of 0.5 mL/min. All sample injections were run in triplicate. Average peak areas before and after treatment for both photocatalytic and photolytic degradation were used for determination of reported degradation percentages and the relative standard deviation. Data was collected and analyzed using Empower Pro software (Waters Corp.) and plotted using Prism 5 (GraphPad Inc., La Jolla, CA).

3. Results and discussion

Surface modification of TiO_2 with affinity peptides imparts a degree of selectivity not traditionally seen in photocatalysis. In this case, TiO_2 particles are modified with SBP to target streptavidin for photocatalytic degradation by illumination with visible light. The discussion progression that follows first proved the affinity function of the hybrid nanoparticle for streptavidin using thin films of SBP–TiO_2, then examined the photocatalytic function of the SBP–TiO_2 while in a colloidal suspension.

3.1. Streptavidin binding peptide (SBP)

The SBP used here, WSHPQFEKGSGSC, consists of the streptavidin *Strep*-tag II recognition sequence, WSHPQFEK, and a flexible linker, GSGSC, that serves to extend the peptide from the TiO_2 particle surface. Experiments were not performed to optimize the length or sequence of the linker. According to online calculators, this 13-mer sequence is approximately 1.6 nm in length [49], with a molecular weight of 1449.5 Da, and an estimated pI = 7.19 [50]. The recognition sequence has the familiar HPQ motif of streptavidin binders, known to occupy the biotin binding cleft [45,51,52]. The dissociation constant, K_D, for *Strep*-tag II has been estimated at 13–72 μM [51], a moderately strong binder to streptavidin.

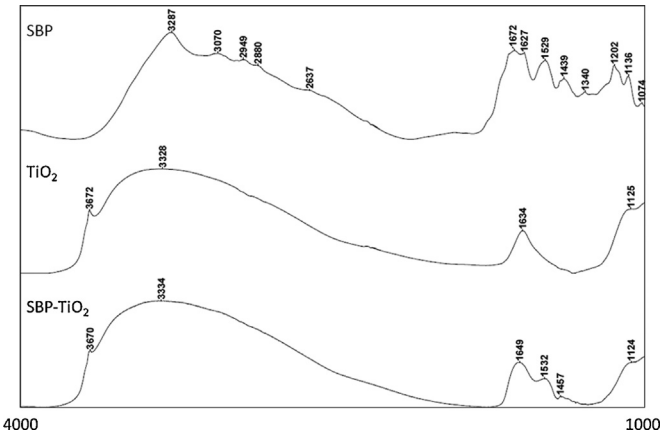

Fig. 2. FTIR spectra of SBP, TiO_2, and SBP–TiO_2.

3.2. TiO_2 modification with SBP

Previous work has shown that monocarboxylate-containing modifiers can bind to undercoordinated titanium atoms to make a surface complex on the nanoparticle through chelating (4-member) or bridging (6-membered) bidentate binding, while enediols can form chelating (5-member) or bridging (7-membered) bidentate binding [30–32,53–57]. This provides a straightforward method for altering the surface chemistry of the titania nanoparticle. Similar to our work with arginine [30], we suspect that the SBP also binds to the TiO_2 through the carboxylate group of the C-terminus. Another carboxylate group is present in the sequence (E, glutamic acid) and the possibility exists that it could also participate in complexation with the TiO_2 surface, although this is less likely since it is an interior residue. Further, if binding does occur at this glutamic acid residue, it is separate from the HPQ motif and it does not appear to interfere with the recognition and affinity of the bound SBP toward streptavidin (*vide infra*).

Attachment of SBP to nanoparticulate TiO_2 and the subsequent function of this hybrid particle are illustrated in the schematic of Fig. 1b. Fig. 1b.i depicts a TiO_2 nanoparticle after modification showing only a single SBP molecule, however, it is expected that the SBP will fill all favorable and accessible surface sites around the nanoparticle. The SBP covalently binds to the TiO_2 surface *via* the carboxylate group at the C-terminus with the N-terminus extending into solution. Surface blocking by BSA occupies and blocks any remaining bare TiO_2 surface. When presented with a combination of biomolecules (Fig. 1b.ii), the HPQ binding motif selectively recognizes and binds the streptavidin in solution, holding it in close proximity to the TiO_2 surface. Illumination of the particle initiates the photocatalytic degradation of molecules at the surface (Fig. 1b.iii), in this case, the streptavidin protein, to by-product molecules that are no longer recognized by the SBP as shown in Fig. 1b.iv. Ideally, other proteins in solution with no affinity to the SBP are not degraded. A similar photocatalytic process is expected at the surface of thin films of SBP–TiO_2 to create a selective affinity and degradation surface.

3.3. Characterization with FTIR

FTIR was performed to verify the presence of SBP at the nanoparticle surface and potentially elucidate the binding interaction. The IR absorbance spectra of solid samples of lyophilized SBP, unmodified TiO_2 nanoparticles, and SBP–TiO_2 are shown offset in Fig. 2. The TiO_2 spectrum is dominated by the broad OH stretching peak from 3600 to 3000 cm^{-1} due to adsorbed water at the surface, the 1634 cm^{-1} OH scissoring band also from

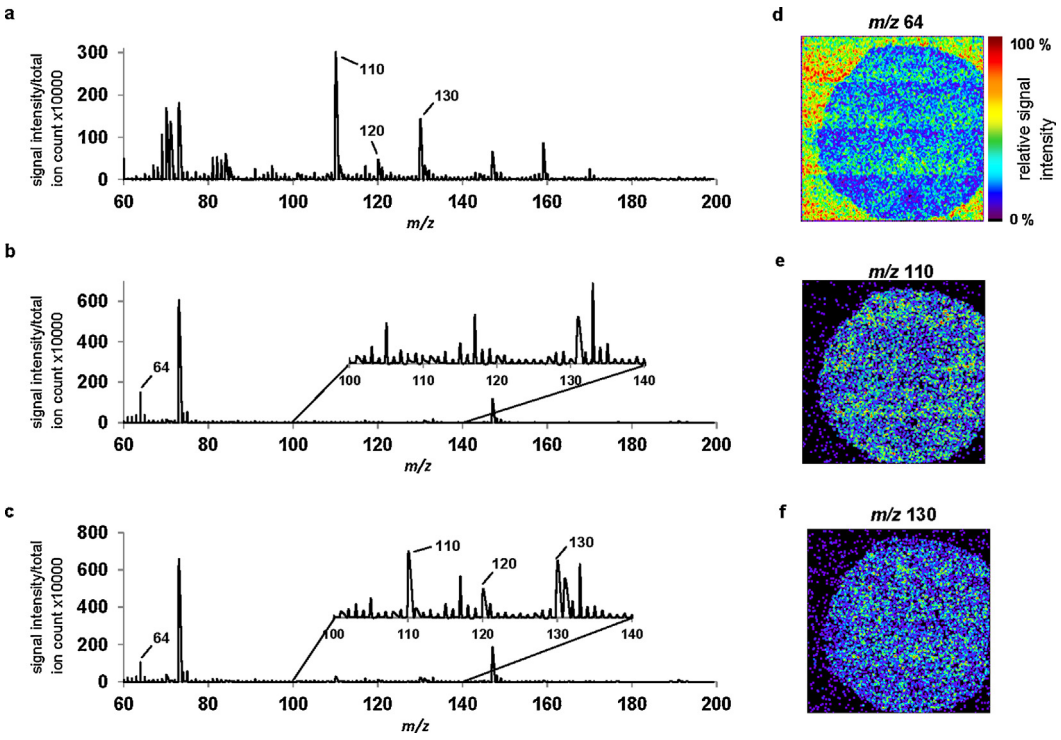

Fig. 3. ToF-SIMS analysis of (a) the lyophilized SBP; (b) the bare TiO_2 thin film surface with expanded inset; and (c) the SBP–TiO_2 thin film surface with expanded inset. (d–f): ToF-SIMS images represent the distribution of different molecular ion species within a SBP–TiO_2 thin film spot; (d) represents TiO (*m*/*z* 64); (e) fragmentation ion of SBP (*m*/*z* 110); (f) fragmentation ion of SBP (*m*/*z* 130). (For interpretation of the references to color in the text, the reader is referred to the web version of this article.)

adsorbed water, and the Ti—O—Ti stretching band that begins to appear toward 1000 cm^{-1} and below [27,58]. SBP is more complicated since the 13-mer peptide includes several different functional groups on the peptide backbone. Likely assignments include the broad N—H (amine) and O—H (serine) stretching in the 3300–3000 cm^{-1} region, C—H stretching peaks (lysine, for instance) in the 3000–2800 cm^{-1} region, and C═O asymmetric (1672 cm^{-1}) and symmetric (1529 cm^{-1}) stretching bands from carboxylate groups (glutamic acid). Comparing the spectra of bare TiO_2 and SBP–TiO_2, surprisingly strong peaks in the C═O stretching region are observed in the latter due to the presence of SBP on the nanoparticles. The shift in the OH scissoring peak from 1634 to 1649 cm^{-1} may be due to disruption of the adsorbed water layer by the SBP. Peaks due to the asymmetric and symmetric stretching of C═O at the surface or interior —COOH groups of glutamic acid are likely hidden by the 1649 cm^{-1} peak and account for the 1532 cm^{-1} peak, respectively. The peaks are slightly shifted from those in pure SBP due to covalent attachment to Ti atoms at the particle surface. The small broad peak at 1457 cm^{-1} in SBP–TiO_2 is possibly due to carboxylate salts (—COOM) that have been previously observed at lower wavelengths [30]. All other SBP peaks due to —NH, —OH, or —CH stretching are not observed, overwhelmed by the large TiOH peak.

Since the SBP–TiO_2 nanoparticles were copiously washed before FTIR analysis, these new peaks are likely not from unbound SBP. It is surprising, however, that the IR peaks associated with the SBP are prominent, since only a monolayer of SBP should remain after covalent attachment and washing steps. The presence of these new peaks demonstrates that the TiO_2 has been modified with a stable layer of SBP.

3.4. ToF-SIMS analysis of SBP modified TiO_2

Evidence for TiO_2 surface modification with SBP is also provided by SIMS data. Liquid metal and cluster ion sources are softer ionization methods resulting in less molecular fragmentation, and are well suited for analyzing biological materials [59,60]. ToF-SIMS spectra of pure lyophilized SBP, an unmodified TiO_2 film, and a SBP–TiO_2 thin film (Fig. 1a, Step iii) are shown in Fig. 3a–c, respectively. SBP (Fig. 3a) produced a molecular ion peak at *m*/*z* 1448 ($M-H^+$) (not shown) and a number of distinct characteristic fragmentation ions (*m*/*z* 110, 120, 130 and 159). None of these peaks are observed from an unmodified TiO_2 thin film surface as shown in Fig. 3b. Conversely, the peak at *m*/*z* 64 from titanium oxide (TiO) is indicative of the TiO_2 layer and is useful to delineate the TiO_2 surface. Analysis of the SBP–TiO_2 surface (Fig. 3c) did not yield an observable peak for the intact SBP molecular ion (*m*/*z* 1448), suggesting the covalent attachment to the TiO_2 surface is quite stable and fragmentation along the peptide backbone is preferred. All of the molecular fragment ions previously identified as signatures of SBP are present (see inset), except for *m*/*z* 159, suggesting that this fragmentation ion is not preferred when bound to the TiO_2 surface. Utilizing the built-in imaging capability of the ToF-SIMS to image the chemical distribution on a surface, Fig. 3d–f illustrate the spot geometry and composition defined in Fig. 1a, Step iii after removal of the PDMS template and a wash step. In Fig. 3d, the peak intensity profile representing titanium oxide (TiO) (*m*/*z* 64) is lower (blue) within the spot where SBP has been deposited and higher (yellow) in the surrounding area that had been protected by the PDMS template. Moreover, the peaks representing molecular fragments of SBP (*m*/*z* 110 and 130) have greater signal intensity (blue) where SBP was deposited within the spot as compared to the surrounding bare TiO_2 surface (black), as shown in Fig. 3e and f. This ToF-SIMS data thus provide alternative corroborating evidence to IR data for the presence of SBP at the TiO_2 surface.

Peptide binding to the TiO_2 surface as a function of SBP solution concentration (1 μM to 5 mM) was investigated using ToF-SIMS by measuring the changes in SBP signal (*m*/*z* 110) integrated across the spot area. The observed increase in signal across this concentration range, shown in Fig. 4, does not fit a simple Langmuir isotherm,

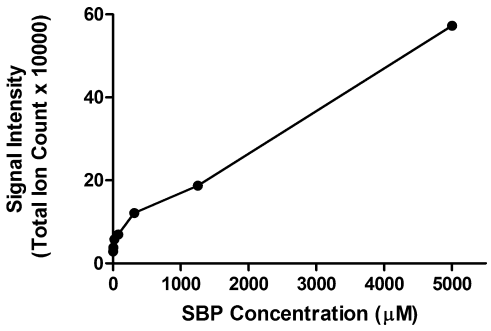

Fig. 4. Relative signal intensity of the SBP specific ion m/z 110 as a function of SBP modification solution concentration showing an increase in relative signal intensity across the SBP concentration range tested.

suggesting that a monolayer of SBP is complete and multilayers are accumulating at the TiO_2 surface as greater SBP concentrations are used in the modification solution. Multilayers of SBP would also explain the relatively large IR absorbances observed for SBP–TiO_2 in Fig. 2.

The two methods described (FTIR and ToF-SIMS) provide strong evidence that the nanoparticle surfaces are modified with the SBP. Further confirmation for the presence of a peptide monolayer is also provided by UV/Vis absorption data (Supplemental information, Fig. S3) where SBP modification causes a red shift in the absorbance of the nanoparticles.

3.5. *Streptavidin binding onto immobilized SBP–TiO_2 surface*

Use of fluorescently labeled antibodies provided an indirect method to demonstrate that immobilized SBP retained its recognition properties for streptavidin with the 5-residue linker likely providing the conformational flexibility needed for affinity, while also showing the BSA blocking capacity. FITC-labeled anti-streptavidin antibodies provide a visual assessment for the spatial location and presence of streptavidin binding at the SBP–TiO_2 surface. BSA is used as a blocking agent to prevent any undesirable non-specific adsorption of proteins to unmodified TiO_2 surfaces. Fig. 5a shows fluorescent images of TiO_2 thin films that were exposed to PBS (i) and BSA (ii), followed by the addition of the FITC-tagged antibody to streptavidin (FITC-anti-strept antibody). An unmodified, unblocked TiO_2 surface (PBS) does slightly adsorb the FITC-anti-strept antibody as shown by the increased fluorescence only within the TiO_2 film spot (Fig. 5a.i). When treated with BSA, however, non-specific adsorption of FITC-anti-strept antibody to the surface is eliminated as seen by the lack of fluorescence within the TiO_2 coated spot (Fig. 5a.ii). This serves to confirm that BSA effectively binds to the TiO_2 to block the surface from FITC-anti-strept antibody. As a final control, a TiO_2 surface was treated with BSA then exposed to streptavidin, followed by the FITC-anti-strept antibody (Fig. 5a.iii). This spot remained dark indicating that BSA is suitable for also preventing non-specific adsorption of the streptavidin. In addition, the presence of streptavidin together in solution with the FITC-anti-strept antibody is also insufficient to cause fluorescence at the TiO_2 surface.

Streptavidin binding as a function of SBP concentration was investigated as described above. Briefly, SBP (0–5 mM) was deposited on TiO_2 thin films, BSA was added to block any remaining unmodified TiO_2 sites, followed by streptavidin, and then finally interrogated with FITC-anti-strept antibody. Increasing the SBP concentration in the solution used to modify the TiO_2 film must bind more streptavidin, as evidenced by the resultant increase in the relative fluorescence intensity from bound FITC-anti-strept antibody (Fig. 5b). This series of images clearly demonstrates the ability of surface bound SBP to bind streptavidin from solution, followed by detection of the sorbed streptavidin with FITC-anti-strept antibody. The relative integrated fluorescence intensity over the TiO_2 spot is plotted in Fig. 5c, where the data is plotted on an arbitrary 0–100% intensity scale, setting the 0 μM SBP relative fluorescence intensity to 0% and the 5 μM SBP relative fluorescence intensity to 100%. The 0 μM added SBP followed by BSA also served as the background, and its fluorescence intensity was subtracted from all other measurements. Increasing concentrations of SBP used to modify the TiO_2 surface result in a sharp increase in streptavidin binding, however, by 1.25 mM SBP, the relative fluorescence intensity plateaus, suggesting either the maximum amount of streptavidin has bound to the surface despite an increasing amount of surface SBP (shown in Fig. 4), or the maximum amount of FITC-anti-strept antibody that can sterically fit at the surface has been reached. The data of Fig. 5c appear to fit a simple Langmuir isotherm, indicating that either a monolayer of streptavidin accumulates at the SBP surface or the FITC-anti-strept antibody is useful to detect only the outermost surface-bound layer of streptavidin. Use of 5 mM SBP solution to modify the TiO_2 surface ensured complete surface coverage of the photocatalyst and was used for the subsequent illumination studies.

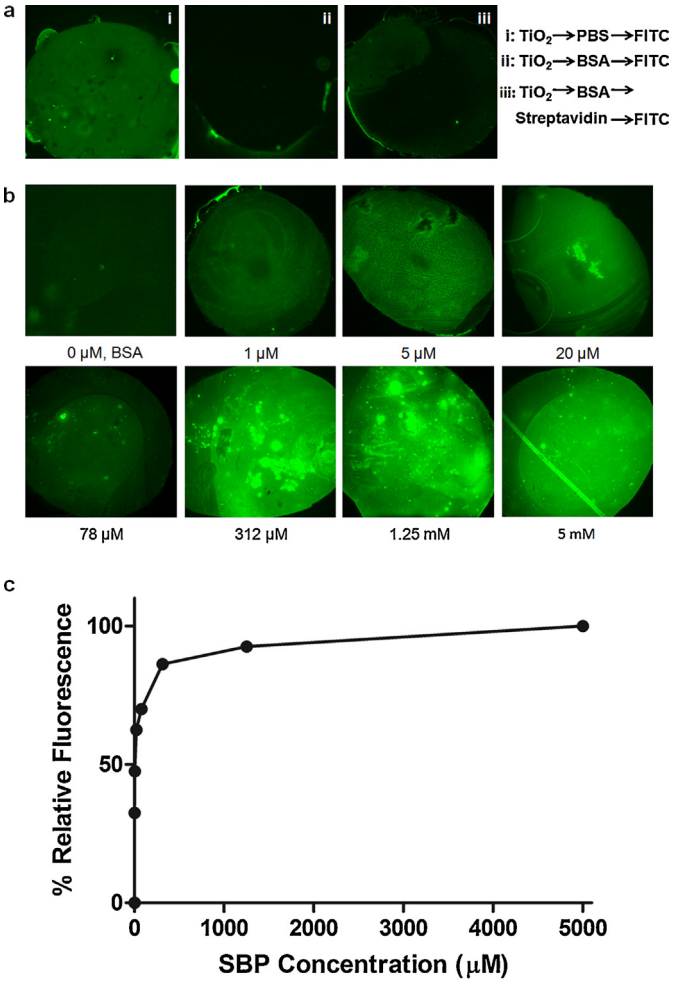

Fig. 5. (a) Fluorescence imaging of a thin film of TiO_2 with (i) added PBS, (ii) added BSA, and (iii) added BSA + streptavidin, followed by the addition of FITC-anti-strept antibody (FITC) to test for non-specific adsorption on the surface. (b) Fluorescence imaging of thin films of TiO_2 with different concentrations of SBP modification solution, followed by the addition of streptavidin and then FITC-anti-strept antibody. (c) Graph of percent relative fluorescence of images from (b). The relative fluorescent intensities of all images have been scaled such that the intensity of 0 μM added SBP is set to 0% and the intensity of 5 mM added SBP is 100%.

a

	i	ii	iii	iv
	SBP-TiO_2	SBP-TiO_2	SBP-TiO_2	TiO_2
BSA	✓	✓	✓	✓
Streptavidin	✓	✓		✓
Illumination	✓	✓	✓	✓
BSA	✓	✓	✓	✓
Streptavidin		✓	✓	
Anti-Streptavidin Antibody (FITC)	✓	✓	✓	✓

b

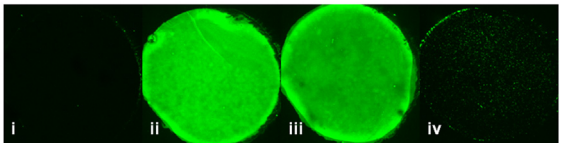

Fig. 6. Stability testing of the SBP–TiO_2 after illumination. (a) Table of experimental steps for cases (i) through (iv) (a checkmark indicates a step occurred). (b) Fluorescent images for cases (i) through (iv) from (a). All illuminations were for 3 h. The fluorescent intensities of all images displayed on the same relative scale.

3.6. Photocatalysis using immobilized SBP–TiO_2

SBP modified TiO_2 thin films were used to investigate the ability to bind and photodegrade streptavidin from solution. Fig. 6a is a summary table of the four conditions (i–iv) tested, with a checkmark indicating that a step was performed and a blank indicating that step was not performed. Fig. 6b shows the fluorescence of the resultant spots after all steps in a condition are complete. Note that the spots are clearly defined and no fluorescence is observed at the unmodified PDMS protected surface outside the spot boundary. The results from each condition are described below.

Condition (i) used an SBP–TiO_2 thin film blocked with BSA to photocatalytically degrade streptavidin with 3 h of illumination. After illumination, BSA was again added to block any new bare TiO_2 that may have developed over time. FITC-anti-strept antibody was then added to the system and the resultant spot (Fig 6b.i) is dark. First, this shows that the initial addition of streptavidin has been photocatalytically degraded and eliminated from the surface, and therefore, the SBP does not inhibit the photocatalytic function of the TiO_2. Second, as expected from Figs. 5a.ii and b, non-specific binding of FITC-anti-strept antibody is undetectable and streptavidin must be present to obtain a fluorescent signal. Since the spot is dark, either all streptavidin within the treatment solution volume has been completely degraded or the SBP is no longer present and functional at the TiO_2 surface.

In condition (ii), an SBP–TiO_2 thin film was used to degrade streptavidin in solution by illuminating for 3 h, but now a second aliquot of streptavidin was added and equilibrated for 2 h, removed, and interrogated with FITC-anti-strept antibody. The resultant film spot is brightly fluorescent (Fig. 6b.ii) indicating that the FITC-anti-strept antibody is bound to streptavidin at the surface. In combination with the result in Fig. 5a.iii, SBP must remain functional and stable as a streptavidin affinity peptide at the surface despite the 3 h illumination. This proves that the covalently bound SBP is a stable, reusable biorecognition agent with the potential for repeated degradation of the target compound.

Condition (iii) probed the stability of the SBP layer against photodegradation by illuminating an SBP–TiO_2 thin film alone for 3 h. The brightly fluorescent spot (Fig. 6b.iii) indicates that the FITC-anti-strept antibody is bound to streptavidin at the surface, proving that the SBP retains its streptavidin recognition function even after long irradiation times in close proximity to the photocatalytic surface.

Condition (iv) used an unmodified TiO_2 film to photocatalytically degrade streptavidin after a 3 h illumination time. A second aliquot of streptavidin was not added. Treatment with FITC-anti-strept antibody shows a dark image, although there is some punctate fluorescence that can be due to non-specific binding of the antibody to bare TiO_2 from incomplete BSA blocking (as seen in Fig. 5a.i), or less likely, unreacted streptavidin remaining at the surface after photocatalysis. In either event, it is clear that streptavidin is not uniformly present across the TiO_2 surface.

Overall, the results show that SBP is bound to the TiO_2 surface in an orientation that allows recognition of streptavidin and the peptide retains its molecular recognition and affinity properties even after illumination. We have previously noted that molecules covalently bound to the TiO_2 surface remain intact despite the photocatalytic processes underway [30–32]. This effect is also observed when tuning the absorption of TiO_2 nanoparticles with surface bound bidentate ligands [61]. The TiO_2 bandgap is altered through electronic coupling of the surface modifier with the nanoparticle conduction band. Illumination of the modified TiO_2 does not degrade the bound ligand. The instantaneous charge separation, the change in the redox properties of the holes localized on the bound SBP ligand, and the conductive nature of the SBP ligand all stabilize the surface layer, yet the particles remain photocatalytically active toward species in solution [62].

3.7. Photocatalytic degradation of proteins in a colloidal solution

The thin film experiments above clearly showed the photocatalytic disappearance of streptavidin from the SBP–TiO_2 surface when illuminated. Photocatalysis was then performed in colloidal SBP–TiO_2 nanoparticle solutions after addition of streptavidin. Fig. 7a shows the chromatograms for several streptavidin solutions and treatment conditions; all traces utilize the same absorbance scale but are offset for clarity. The black trace is the analysis of a 3 mg/mL solution of streptavidin showing a single peak due to streptavidin at a retention time of 18.6 min, labeled as peak 1. A 3 mg/mL streptavidin solution was illuminated for 3 h in the absence of any photocatalyst to determine the extent of photolysis (red trace). Quantification of the peak area indicates that streptavidin is stable under these illumination conditions with no appreciable loss of the streptavidin and without the production of any photolytic by-products.

TiO_2 was added to the 3 mg/mL streptavidin solution to make a 0.1 M TiO_2 colloidal suspension and illuminated. The streptavidin was completely degraded (99.9% ± 0.1%) after 3 h with no visible by-products (green trace). In this instance, three possibilities exist: (1) similar to other organic compounds, streptavidin is completely mineralized to carbon oxides and nitrogen oxides; (2) streptavidin is degraded to by-products that do not absorb at 280 nm; or (3)

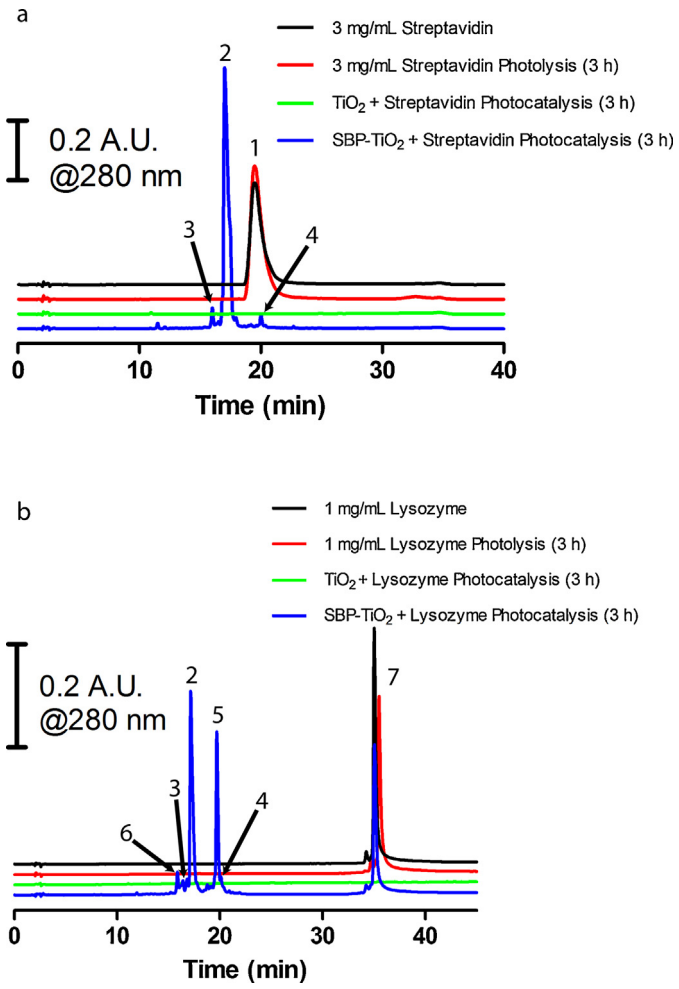

Fig. 7. (a) Chromatographic separations of streptavidin solutions without illumination (black), photolyzed (red), photocatalyzed with bare TiO_2 (green), and photocatalyzed with SBP–TiO_2 (blue). Concentration for streptavidin was 3 mg/mL, and all samples were illuminated for 3 h. (b) Chromatographic separations of lysozyme solutions without illumination (black), photolyzed (red), photocatalyzed with bare TiO_2 (green), and photocatalyzed with SBP–TiO_2 (blue). Concentration for lysozyme was 1 mg/mL, and all samples were illuminated for 3 h. (For interpretation of the references to color in this figure legend, the reader is referred to the web version of this article.)

streptavidin is degraded to by-products that do not elute within this time frame. While analysis of the complete mechanism of streptavidin degradation was not the goal of this research, we suspect that the true mechanism is a combination of these possibilities, with the production of smaller by-product fragments that cannot be readily determined using liquid chromatography and might even be irretrievably lost on the column during analysis. The loss of streptavidin from solution is not simply due to adsorption from solution onto the catalyst particles since streptavidin is lost from the thin film when illuminated (Fig. 6a.iv). These data serve to illustrate that TiO_2 is very effective at streptavidin degradation, including by-products, due to non-specific targeting of surface proximal species.

Addition of SBP–TiO_2 to the 3 mg/mL streptavidin solution to make a 0.1 M SBP–TiO_2 colloidal suspension followed by illumination produces the peaks shown on the blue trace in Fig. 7a. The SBP–TiO_2 photocatalyst is also effective in degrading the streptavidin during the 3 h illumination as shown by the disappearance of the streptavidin peak (99.9% ± 0.1%). Again, this is not due to streptavidin adsorption from solution onto the particles (Fig. 6a.i). A new major peak, however, has appeared at a retention time of 16.7 min (labeled as peak 2) that is not produced under any other condition. In addition, several less abundant by-products are also observed (labeled as peaks 3 and 4) as well as small shoulders on peak 2. Analysis of the SBP solution determined that peak 2 is free SBP, peak 3 is a minor unknown species present in the SBP solution, and peak 4 is an SBP aggregate, most likely dimers due to disulfide formation through the C-terminal cysteines (see Supplemental information). None of these peaks is a streptavidin by-product. Based on the lack of substantial by-products in either chromatographic trace, the SBP–TiO_2 photocatalyst is as effective for complete degradation of the target streptavidin as the bare TiO_2. In this case, it appears that reaction intermediates also have affinity to SBP and are degraded since no by-products were observed. It is possible, however, that a target compound can be degraded to an intermediate that has no affinity to the surface peptide resulting in the accumulation of a non-target by-product.

Fig. 7b displays the chromatographic analysis of solutions from lysozyme degradation. Lysozyme is a 14 kDa protein, smaller than streptavidin, and should be less restricted in reaching the nanoparticle surface for photocatalytic degradation. Lysozyme elutes at 34 min ± 0.5 min and is denoted as peak 7 (black trace) in Fig. 7b. Unlike streptavidin, there is an appreciable loss of lysozyme (approximately 22% ± 6%) due to photolysis during a 3 h illumination period (red trace) but no new photolytic by-product peaks are noted. Wu et al. [63] suggested that since lysozyme has six tryptophan residues and four pairs of disulfide bridges, this is likely due to tryptophan-mediated reduction of internal disulfide bonds with the possibility of intermolecular dimerization. We note that streptavidin has no internal cysteine residues or disulfide bridges [64] which may explain its relative photolytic stability. But similar to streptavidin, the lysozyme is completely degraded (99.8% ± 0.1%) when illuminated in the presence of bare TiO_2 (green trace) and again, no by-products are observed. These losses can be compared to the loss of lysozyme under photocatalytic conditions in the presence of the SBP–TiO_2. A peak area analysis shows a 36% ± 6% loss of lysozyme under photocatalytic conditions with SBP–TiO_2 (blue trace, Fig. 7b). This loss would include both photolytic and photocatalytic mechanisms, thus, only about 14% of the lysozyme is degraded photocatalytically with SBP–TiO_2. Further, it produces a large by-product (Peak 5, 18.8 min) and a much less abundant by-product (Peak 6, 15.0 min). These peaks are different from peaks 3 and 4 in Fig. 7a and are not SBP background peaks. Peaks 2, 3, and 4 are identical to those in Fig. 7a and originate from the SBP in solution. The results indicate that (1) the SBP acts to inhibit the photocatalytic degradation of non-target proteins, *i.e.*, lysozyme; (2) the SBP restricts lysozyme access to the TiO_2 surface; (3) the photocatalytic by-products of lysozyme are also non-target molecules and their degradation is also retarded by the SBP–TiO_2; and (4) the SBP layer itself does not degrade over this illumination time otherwise the lysozyme would be degraded at the resulting bare TiO_2 surface.

The SBP clearly acts to provide selectivity to the photocatalytic process. The target streptavidin is efficiently and completely degraded while the degradation of a non-target protein, lysozyme, is substantially retarded. The photocatalysis of lysozyme that does occur with SBP–TiO_2 may be due to a slight affinity of SBP toward lysozyme. This would result in weak attraction and an increase in residence time for the lysozyme within the reaction zone surrounding the modified TiO_2 nanoparticles, leading to the observed slow and limited photocatalysis of lysozyme. Similarly, the lysozyme by-product (peak 5) is expected to have low to no affinity to SBP and, hence, it is also resistant to this targeted photocatalysis and would accumulate in solution. More selectivity can be introduced by selecting a recognition peptide that has been engineered not only for target affinity but also for negative selectivity toward non-target molecules. Degradation of lysozyme with SBP–TiO_2 may result from accessible regions of unmodified titania, although the

lack of any by-product (*i.e.*, peaks 5 and 6) in the bare TiO_2 trace supports the idea that these two photocatalysts (SBP–TiO_2 *vs.* bare TiO_2) employ two different mechanisms. These results also strongly suggest that the SBP affinity layer on the TiO_2 can act to prevent surface poisoning by providing a chemical barrier against all non-target compounds, including by-products, that might otherwise react with and passivate the TiO_2 surface.

A 3 h illumination time was chosen in these experiments to accentuate the ability of SBP to alter the selectivity of the photocatalytic process, not to compare kinetics. Since the SBP surface layer dictates the interaction of target molecules with the photocatalyst while bare TiO_2 has only mass transfer limitations, it is quite likely that the reaction kinetics for bare TiO_2 is faster than the SBP–TiO_2 for streptavidin degradation. A faster photocatalyst was not the goal here, however, but one that provides a level of selectivity for biomolecular degradation. A closer study of the photocatalytic degradation mechanism of streptavidin using the SBP–TiO_2, its reuse capability and lifetime, and prevention of surface poisoning are goals of further research.

4. Conclusion

The surface of TiO_2 nanoparticles is covalently modified with a streptavidin binding peptide (SBP) using a simple linking method that takes advantage of the carboxylate terminus of the peptide and the undercoordinated titanium atoms at the particle surface. This affinity peptide imparts selectivity in binding and, when illuminated, photocatalytic degradation of its cognate protein target, streptavidin, while substantially diminishing the degradation of a non-target protein, lysozyme. This selectivity function was demonstrated in both a colloidal suspension of the modified catalyst and as a thin photocatalyst film. Photocatalytic selectivity is likely limited by the selectivity of the recognition peptide. Engineering the peptide for better target affinity and lower disassociation rates, as well as decreased affinity for non-target molecules, is predicted to lead to better photocatalytic degradation selectivity. In fact, the primary strength of this hybrid nanoparticle over other selectivity methods (*e.g.*, molecular imprinting) is the flexibility and fine tuning available simply by changing the peptide sequence for affinity to other small molecules. Importantly, the immobilized SBP is not photocatalytically degraded when covalently bound to the TiO_2 surface but this resistance does not extend to the cognate target. Further, it retains its ability to bind streptavidin even after illumination, demonstrating a stable surface layer with resistance to by-product (non-target) poisoning and the potential for reuse and recycle. This study demonstrates the ability to modify TiO_2 with affinity peptides to promote photocatalytic selectivity toward a target protein with minimal degradation of non-target compounds. The low cost of TiO_2, the relatively low cost of small peptides, and the inexpensive source of illumination (sunlight) all bode well for larger scale applications. It is anticipated that these hybrid photocatalysts will have utility in selective removal of desired proteins and biomolecules from complex media and mixtures, including biological fluids, pharmaceuticals, wastewater, and ecological systems.

Conflict of interest

Authors report no conflict of interest.

Acknowledgements

We thank Timothy Spila for his assistance with the ToF-SIMS. Research was carried out in part in the Frederick Seitz Materials Research Laboratory Central Facilities, University of Illinois at Urbana-Champaign. This research was funded by the Defense Threat Reduction Agency (DTRA), grant number BRCALL07-E-2-0035.

Appendix A. Supplementary data

Supplementary data associated with this article can be found, in the online version, at http://dx.doi.org/10.1016/j.apcatb.2015.03.060.

References

[1] C.G. Wu, L.F. Tzeng, Y.T. Kuo, C.H. Shu, Appl. Catal. A 226 (2002) 199–211.
[2] S. Kwon, M. Fan, A.T. Cooper, H. Yang, Crit. Rev. Env. Sci. Technol. 38 (2008) 197–226.
[3] M.A. Fox, M.T. Dulay, Chem. Rev. 93 (1993) 341–357.
[4] A. Wold, Chem. Mater. 5 (1993) 280–283.
[5] A. Mills, R.H. Davies, D. Worsley, Chem. Soc. Rev. 22 (1993) 417–425.
[6] M.R. Hoffmann, S.T. Martin, W. Choi, D.W. Bahnemann, Chem. Rev. 95 (1995) 69–96.
[7] S.Y. Lee, S.J. Park, J. Ind. Eng. Chem. 19 (2013) 1761–1769.
[8] H. Park, Y. Park, W. Kim, W. Choi, J. Photochem. Photobiol. C 15 (2013) 1–20.
[9] A. Klapproth, S. Linnemann, D. Bahnemann, R. Dillert, G. Fels, J. Labelled Compd. Radiopharm. 41 (1998) 337–343.
[10] H.S. Son, S.J. Lee, I.H. Cho, K.D. Zoh, Chemosphere 57 (2004) 309–317.
[11] D.C. Schmelling, K.A. Gray, P.V. Kamat, Environ. Sci. Technol. 30 (1996) 2547–2555.
[12] L. Le Campion, C. Giannotti, J. Ouazzani, Chemosphere 38 (1999) 1561–1570.
[13] E. Pelizzetti, C. Minero, P. Piccinini, M. Vincenti, Coord. Chem. Rev. 125 (1993) 183–193.
[14] Y.H. Ngo, D. Li, G.P. Simon, G. Garnier, Adv. Colloid Interface 163 (2011) 23–38.
[15] S. Lu, D. Wu, Q. Wang, J. Yan, A.G. Buekens, K. Cen, Chemosphere 82 (2011) 1215–1224.
[16] R.J. Berry, M.R. Mueller, Microchem. J. 50 (1994) 28–32.
[17] L.R. Skubal, N.K. Meshkov, J. Photochem. Photobiol. A 148 (2002) 211–214.
[18] L.R. Skubal, N.K. Meshkov, T. Rajh, M. Thurnauer, J. Photochem. Photobiol. A 148 (2002) 393–397.
[19] I.A. Ruvarac-Bugarčicí, Z.V. Šaponjicí, S. Zec, T. Rajh, J.M. Nedeljkovic, Chem. Phys. Lett. 407 (2005) 110–113.
[20] P.K.J. Robertson, J.M.C. Robertson, D.W. Bahnemann, J. Hazard. Mater. 211–212 (2012) 161–171.
[21] T. Matsunaga, R. Tomada, T. Nakajima, H. Wake, FEMS Microbiol. Lett. 29 (1985) 211–214.
[22] C. Hu, J. Guo, J. Qu, X. Hu, Langmuir 23 (2007) 4982–4987.
[23] N. Baram, D. Starosvetsky, J. Starosvetsky, M. Epshtein, R. Armon, Y. Ein-Eli, Appl. Catal. B 101 (2011) 212–219.
[24] A.R. Almeida, J.T. Carneiro, J.A. Moulijn, G. Mul, J. Catal. 273 (2010) 116–124.
[25] Y. Paz, C.R. Chim. 9 (2006) 774–787.
[26] C. Ogino, K. Kanehira, R. Sasai, S. Sonezaki, N. Shimizu, J. Biosci. Bioeng. 104 (2007) 339–342.
[27] H. Jia, W.J. Xiao, L. Zhang, Z. Zheng, H. Zhang, F. Deng, J. Phys. Chem. C 112 (2008) 11379–11384.
[28] T. Rajh, A.E. Ostafin, O.I. Micic, D.M. Tiede, M.C. Thurnauer, J. Phys. Chem. 100 (1996) 4538–4545.
[29] S. Li, F. Zheng, X. Liu, F. Wu, N. Deng, J. Yang, Chemosphere 61 (2005) 589–594.
[30] O.V. Makarova, T. Rajh, M.C. Thurnauer, A. Martin, P.A. Kemme, D. Cropek, Environ. Sci. Technol. 34 (2000) 4797–4803.
[31] D. Cropek, P.A. Kemme, O.V. Makarova, L.X. Chen, T. Rajh, J. Phys. Chem. C 112 (2008) 8311–8318.
[32] W.-Y. Ahn, S.A. Sheeley, T. Rajh, D.M. Cropek, Appl. Catal. B 74 (2007) 103–110.
[33] L. Shun-Xing, Z. Feng-Ying, C. Wen-Lian, H. Ai-Qin, X. Yu-Kun, J. Hazard. Mater. 135 (2006) 431–436.
[34] K.T. Ranjit, I. Willner, S. Bossmann, A. Braun, Res. Chem. Intermed. 25 (1999) 733–756.
[35] X. Zhang, F. Wu, N. Deng, J. Hazard. Mater. 185 (2011) 117–123.
[36] S. Ghosh-Mukerji, H. Haick, Y. Paz, J. Photochem. Photobiol. A 160 (2003) 77.
[37] J. Matos, J. Laine, J.M. Herrmann, Appl. Catal. B 18 (1998) 281–291.
[38] X. Zhang, X. Li, Q. Zhang, J. Yang, N. Deng, Catal. Commun. 16 (2011) 7–10.
[39] K. Inumaru, M. Murashima, T. Kasahara, S. Yamanaka, Appl. Catal. B 52 (2004) 275–280.
[40] X. Shen, L. Zhu, J. Li, H. Tang, Chem. Commun. (2007) 1163–1165.
[41] S.W. Lee, I. Ichinose, T. Kunitake, Langmuir 14 (1998) 2857–2863.
[42] H. Huang, J. Zhou, H. Liu, Y. Zhou, Y. Feng, J. Hazard. Mater. 178 (2010) 994–998.
[43] R.C. Thompson, Inorg. Chem. 23 (1984) 1794–1798.
[44] J.D. Ellis, A.G. Sykes, J. Chem. Soc. (1973) 537–543.
[45] T.G.M. Schmidt, J. Koepke, R. Frank, A. Skerra, J. Mol. Biol. 255 (1996) 753–766.
[46] S.V. Babu, M. David, R.C. Patel, Appl. Opt. 30 (1991) 839–846.
[47] Z.V. Šaponjicí, T. Rajh, J.M. Nedeljkovicí, M.C. Thurnauer, Mater. Sci. Forum 352 (2000) 91–95.
[48] W.S. Rasband, ImageJ, U.S. National Institutes of Health, Bethesda, Maryland, USA, http://imagej.nih.gov/ij/, 1997–2014.
[49] http://www.calctool.org/CALC/prof/bio/protein_size

[50] http://protcalc.sourceforge.net
[51] D.S. Wilson, A.D. Keefe, J.W. Szostak, Proc. Natl. Acad. Sci. U. S. A 98 (2001) 3750–3755.
[52] J.J. Rice, A. Schohn, P.H. Bessette, K.T. Boulware, P.S. Daugherty, Protein Sci. 15 (2006) 825–836.
[53] C.B. Mendive, T. Bredow, M.A. Blesa, D.W. Bahnemann, Phys. Chem. Chem. Phys. 8 (2006) 3232–3247.
[54] D. Gutiérrez-Tauste, X. Domènech, C. Domingo, J.A. Ayllón, Thin Solid Films 516 (2008) 3831–3835.
[55] B. Geiseler, L. Fruk, J. Mater. Chem. 22 (2012) 735–741.
[56] L. de la Garza, Z.V. Saponjic, N.M. Dimitrijevic, M.C. Thurnauer, T. Rajh, J. Phys. Chem. B 110 (2006) 680–686.
[57] S.J. Hug, D. Bahnemann, J. Electron. Spectrosc. 150 (2006) 208–219.
[58] G.L. Wang, J.J. Xu, H.Y. Chen, Biosens. Bioelectron. 24 (2009) 2494–2498.
[59] K.R. Amaya, J.V. Sweedler, D.F. Clayton, J. Neurochem. 118 (2011) 499–511.
[60] M. Wilhelmi, C. Müller, C. Ziegler, M. Kopnarski, Anal. Bioanal. Chem. 400 (2011) 697–701.
[61] T. Rajh, L.X. Chen, K. Lukas, T. Liu, M.C. Thurnauer, D.M. Tiede, J. Phys. Chem. B 106 (2002) 10543–10552.
[62] T. Rajh, N.M. Dimitrijevic, M. Bissonnette, T. Koritarov, V. Konda, Chem. Rev. 114 (2014) 10177–10216.
[63] L.Z. Wu, Y.B. Sheng, J.B. Xie, W. Wang, J. Mol. Struct. 882 (2008) 101–106.
[64] T. Sano, S. Vajda, G.O. Resnik, C.L. Smith, C.R. Cantor, Ann. N.Y. Acad. Sci. 799 (1996) 383–390.